New Precise Value for the Muon Magnetic Moment and Sensitive Test of the Theory of the hfs Interval in Muonium*

D. E. Casperson, T. W. Crane, A. B. Denison, P. O. Egan, V. W. Hughes, F. G. Mariam, H. Orth,† H. W. Reist, P. A. Souder, R. D. Stambaugh, P. A. Thompson, and G. zu Putlitz

University of Bern, Bern, Switzerland, and University of Heidelberg, Heidelberg, West Germany, and Los Alamos Scientific Laboratory, Los Alamos, New Mexico 87545, and University of Wyoming, Laramie, Wyoming 82071, and Yale University, New Haven, Connecticut 06520

(Received 15 March 1977)

Measurements of Zeeman transitions in the ground state of muonium at strong magnetic field have yielded values for the hfs interval, $\Delta\nu = 4463\,302.35(52)$ kHz (0.12 ppm) and for the muon magnetic moment, $\mu_\mu/\mu_p = 3.183\,3403(44)$ (1.4 ppm), of considerably higher precision than previous results. The theoretical expression for $\Delta\nu$, including our measured value of μ_μ/μ_p, disagrees with the experimental value by 2.5 standard deviations. The electronic g_J density shift for muonium in Kr has been measured.

A principal motivation for muonium (μ^+e^-) experiments has been to test the conventional quantum electrodynamic description of the μ-e interaction.[1,2] A precise comparison of experiment and theory for the muonium hyperfine structure interval $\Delta\nu$ has thus far been significantly limited by uncertainties in the values of the fine-structure constant α and of the muon magnetic moment μ_μ. Recently α has been determined with much higher precision.[3] In this Letter we report on an experiment performed at the Clinton P. Anderson Meson Physics Facility (LAMPF) which simultaneously determined $\Delta\nu$ and μ_μ to higher precision by measuring two Zeeman transitions in muonium at strong magnetic field. Hence we are now able to test with more sensitivity the agreement between experimental and theoretical values for $\Delta\nu$.

The experiment utilized the microwave magnetic resonance technique[4-6] to measure the frequencies for the transitions $(M_J, M_\mu) = (\frac{1}{2}, \frac{1}{2}) \leftrightarrow (\frac{1}{2}, -\frac{1}{2})$, designated ν_{12}, and $(-\frac{1}{2}, -\frac{1}{2}) \leftrightarrow (-\frac{1}{2}, +\frac{1}{2})$, designated ν_{34}, at a strong static magnetic field of 13.6 kG. The transition frequencies are given by

$$\nu_{12} = \frac{+\mu_B{}^\mu g_\mu{}'H}{h} + \frac{\Delta\nu}{2}[(1+x) - (1+x^2)^{1/2}], \tag{1}$$

$$\nu_{34} = \frac{-\mu_B{}^\mu g_\mu{}'H}{h} + \frac{\Delta\nu}{2}[(1-x) + (1+x^2)^{1/2}], \tag{2}$$

where $x = (g_J\mu_B{}^e - g_\mu{}'\mu_B{}^\mu)H/(h\Delta\nu)$; $\mu_B{}^\mu$ ($\mu_B{}^e$) is the muon (electron) Bohr magneton; $g_\mu{}' = g_\mu(1-\alpha^2/3)$ is the muon g value in μ^+e^- and g_μ is the free-muon g value; g_J is the electron g value in μ^+e^-. To obtain $\Delta\nu$ and μ_μ we combine Eqs. (1) and (2) to give

$$\nu_{12} + \nu_{34} = \Delta\nu, \tag{3}$$

$$\nu_{34} - \nu_{12} = -2\mu_B{}^\mu g_\mu{}'H/h + \Delta\nu[(1+x^2)^{1/2} - x]. \tag{4}$$

The experimental arrangement is shown in Fig. 1. With the LAMPF 800-MeV proton beam at 100 μA average intensity (6% duty factor) and the stopped-muon channel tuned for 48-MeV/c muons, a stopping rate of 2.5×10^4 μ^+/sec was obtained in a 0.2-g/cm^2 (1.7 atm) krypton gas target. The logic signals for stopping muons and decay positrons are derived from plastic scintillators and proportional wire chambers.[7] A high-precision eighth-order solenoid electromagnet[8] with iron shielding provided a 13.6-kG magnetic field stable to better than 1 ppm and homogeneous to ~5

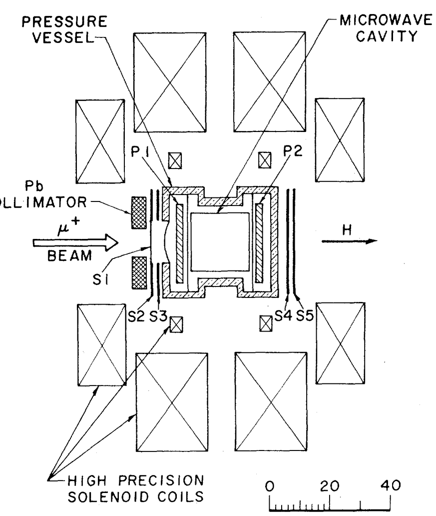

FIG. 1. Schematic diagram of the experimental setup. $P1$ and $P2$ are Ar-CO_2 proportional chambers. $S1$ through $S5$ are plastic scintillation counters. A muon stopping in the active region of the target is defined as $\mu_S = S1 \circ P1 \circ \overline{P2}$. A forward decay positron is defined as $e_F = S4 \circ S5 \circ P2 \circ \overline{P1}$ and a backward positron as $e_B = S2 \circ S3 \circ P1 \circ \overline{P2}$. Iron shielding around the precision solenoid is omitted for clarity.

ppm over the active region. The magnet was powered by a highly stable 1-MW supply, and the current was regulated to lock the field to a proton NMR probe located at the outer diameter of the microwave cavity. The field at the center of the cavity was measured daily with an insertable NMR probe, and no significant changes in the offset of the field at the cavity center relative to the locking probe were seen. Detailed field maps of the cavity region were made periodically, and no significant changes in the field distribution or homogeneity were noted. The microwave cavity was resonant in the TM_{110} mode at 1.918 GHz (ν_{12} at 13.6 kG) and in the TM_{210} mode at 2.545 GHz (ν_{34}), and was excited with an input power of ~50 W switched on and off at 3 Hz, alternating between modes for successive microwave on periods.

To obtain a resonance curve the microwave powers and frequencies were fixed and the magnetic field, H, was varied over 21 values with data taken for ~10 min at each field. For each field value and each transition frequency, both a forward and backward signal are calculated. The signals are defined as

$$S=\left[\frac{(e/\mu_S)_{\text{rf on}}}{(e/\mu_S)_{\text{rf off}}}-1\right]\times 100\%.$$

A resonance curve is shown in Fig. 2 where a least-squares fit to the theoretical line shape[4,5] is also shown. Data were taken at Kr densities of 1.7 and 5.3 atm, with the bulk of the data concentrated at the lower density. The krypton density was determined to 0.5% from measurements of the gas pressure with a quartz Bourdon-tube gauge and the gas temperature with thermocouples. In all, about forty resonance curves as typified by the curves shown in Fig. 2 were taken for each transition frequency.

Analysis began with the fitting of a Lorentzian (in H) line shape to the data of a resonance curve. Correction for the exact dependence of the line shape on the external field was found to shift the initially fitted line centers by only 1 part in 10^3 of the linewidth. In addition, corrections due to the static magnetic field distribution over the cavity, the muon stopping distributions (measured separately with a small movable scintillation counter), the microwave power distribution, and the change of analyzing power with static magnetic field were made in the line-shape analysis and altogether shifted the line center by about 1 part in 10^3 of the linewidth. The values for ν_{12} and ν_{34} obtained at each density were fitted by a linear density shift

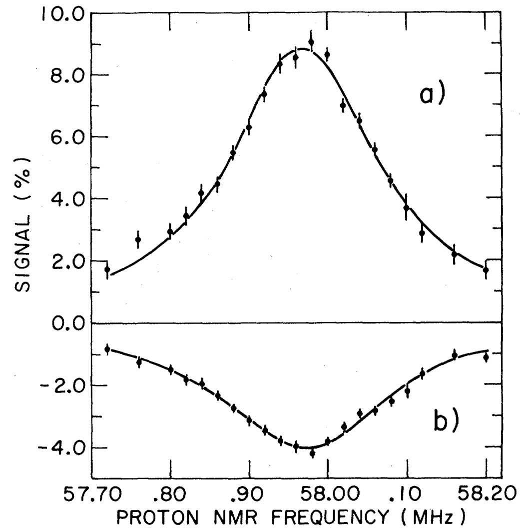

FIG. 2. A resonance line for transition ν_{12} in a 1.7-atm Kr target, for (a) backward and (b) forward positron decay. The solid line is a least-squares fit of a Lorentzian curve to the data. The linewidth is 55 G and arises from the muon decay and power broadening. The data shown were obtained in 11 h.

equation, $\nu(D)=\nu(0)(1+aD)$, after a small correction (2 parts in 10^7 at 5.3 atm) was made for the known quadratic density dependence.[7] The results of the density fits are

$$\begin{aligned}&\nu_{12}(0)=1917\,654.15(33)\text{ kHz},\\&a_{12}=-16.211(80)\text{ kHz/atm (Kr},0^\circ\text{C)};\\&\nu_{34}(0)=2545\,648.20(36)\text{ kHz},\\&a_{34}=-19.779(86)\text{ kHz/atm (Kr},0^\circ\text{C)}.\end{aligned}\tag{5}$$

The zero-density values of ν_{12} and ν_{34} may be combined, with the use of Eqs. (3) and (4), to yield

$$\Delta\nu=4463\,302.35(52)\text{ kHz (0.12 ppm)},\tag{6}$$

$$\mu_\mu/\mu_p=3.183\,3403(44)\text{ (1.4 ppm)},\tag{7}$$

where the errors are predominantly from counting statistics. The value of $\Delta\nu$ is more precise by a factor of 3 to 4 than earlier measurements[7,9] from very-weak-field transitions and agrees with these values. Our value of μ_μ/μ_p agrees with the less precise value of $\mu_\mu/\mu_p=3.183\,3467(82)$ (2.6 ppm), measured by muon spin precession in liquids[10] (principally H_2O), and the two values give a weighted average of

$$\mu_\mu/\mu_p=3.183\,3417(39)\text{ (1.2 ppm)}.\tag{8}$$

The current theoretical value for $\Delta\nu$ based on conventional muon electrodynamics is[2,11]

$$\Delta\nu_{\text{theo}} = (\tfrac{16}{3}\alpha^2 c R_\infty \mu_\mu/\mu_B{}^e)(1+m_e/m_\mu)^{-3}(1+\tfrac{3}{2}\alpha^2+a_e+\epsilon_1+\epsilon_2+\epsilon_3-\delta_\mu'), \tag{9}$$

where

$$a_e = \alpha/2\pi - 0.328\,48\alpha^2/\pi^2 + (1.195\pm0.026)\alpha^3/\pi^3;\quad \epsilon_1 = \alpha^2(\ln 2 - \tfrac{5}{2});$$

$$\epsilon_2 = -(8\alpha^3/3\pi)\ln\alpha\,(\ln\alpha - \ln 4 + \tfrac{281}{480});\quad \epsilon_3 = (\alpha^3/\pi)(18.4\pm5);$$

$$\delta_\mu' = \frac{m_e}{m_\mu}\left\{\frac{3\alpha}{\pi}\left[1-\left(\frac{m_e}{m_\mu}\right)^2\right]^{-1}\ln\frac{m_\mu}{m_e} + \frac{9}{2}\alpha^2\ln\alpha\left[1+\left(\frac{m_e}{m_\mu}\right)\right]^{-2}\right\};$$

in which[12]

$$\alpha^{-1} = 137.035\,987(29)\ (0.21\text{ ppm});\quad R_\infty = 1.097\,373\,143(10)\times10^5\text{ cm}^{-1}\ (0.01\text{ ppm});$$

$$c = 2.997\,924\,58(1.2)\times10^{10}\text{ cm/sec}\ (0.004\text{ ppm});\quad \mu_\mu/\mu_B{}^e = (\mu_\mu/\mu_p)\mu_p/\mu_B{}^e; \tag{10}$$

$$\mu_p/\mu_B{}^e = 1.521\,032\,209(16)\times10^{-3}\ (0.01\text{ ppm});\quad m_\mu/m_e = 206.768\,18(54)\ (2.6\text{ ppm}).$$

Hence

$$\Delta\nu_{\text{theo}} = (\mu_\mu/\mu_p)(1.402\,085\,89\pm0.8\text{ ppm})\times10^6\text{ kHz}. \tag{11}$$

Using μ_μ/μ_p from Eq. (8) yields

$$\Delta\nu_{\text{theo}} = 4463\,318.5(6.5)\text{ kHz (1.5 ppm)}, \tag{12}$$

in which the uncertainty arises from the 1.2 ppm error in μ_μ/μ_p and the 0.6 ppm estimate of the theoretical error in the evaluation of ϵ_3.[11] The difference

$$\Delta\nu_{\text{theo}} - \Delta\nu_{\text{expt}} = 16.1(6.6)\text{ kHz (1.5 ppm)} \tag{13}$$

is 2.5 standard deviations of the combined error. In view of this discrepancy, it seems particularly important to re-examine the ϵ_3 term and other higher-order radiative and relativistic recoil terms contributing to $\Delta\nu$.[13,14] An exotic interaction arising from a neutral-current weak interaction would require a coupling constant about 100 times that predicted by the Weinberg-Salam model to remove the discrepancy.[15] A coupling of muonium to antimuonium with the Fermi coupling constant would alter $\Delta\nu_{\text{theo}}$ by about 4 kHz.

Our measurement of μ_μ/μ_p can be used to obtain the most precise value for the muon-electron mass ratio,

$$\frac{m_\mu}{m_e} = \frac{\mu_p}{\mu_\mu}\frac{\mu_e}{\mu_p}\frac{|g_\mu|}{|g_e|} = 206.768\,59(29)\quad (1.4\text{ ppm}), \tag{14}$$

where $g_\mu = -2[1.001\,165\,895(27)]$ (0.027 ppm).[12,16]

Finally, the measured density dependences of ν_{12} and ν_{34}, Eq. (5), indicate a density dependence of g_J, in addition to the well-known hfs density shift of $\Delta\nu$. We neglect any density dependence of g_μ', which should be an excellent approximation. The measured density shifts (for Kr, 0°C) are

$$\frac{1}{\Delta\nu}\frac{\partial\Delta\nu}{\partial D} = -10.610(34)\times10^{-9}\text{ Torr}^{-1},$$

$$\frac{1}{g_J}\frac{\partial g_J}{\partial D} = -3.05(60)\times10^{-9}\text{ Torr}^{-1}. \tag{15}$$

This latter value does not agree well with another determination from a strong-field muonium experiment.[17]

We are happy to acknowledge important contributions to this experiment by A. Disco, S. Dhawan, R. Fong-Tom, and I. Winters of Yale University and by E. Schneider of LAMPF, and also the support of the LAMPF operating staff.

*Research (Yale University Report No. COO-3075-163) supported in part by the U. S. Energy Research and Development Administration under Contract No. EY-76-C-02-3075 and Los Alamos Scientific Laboratory, Los Alamos, N. Mex. 87545.

†Max Kade Fellow.

[1]V. W. Hughes, Annu. Rev. Nucl. Sci. 16, 445 (1966).

[2]S. J. Brodsky and S. D. Drell, Annu. Rev. Nucl. Sci. 20, 147 (1970).

[3]P. T. Olsen and E. R. Williams, *Atomic Masses and Fundamental Constants 5*, edited by J. H. Sanders and A. H. Wapstra (Plenum, New York, 1976), p. 538.

[4]J. M. Bailey *et al.*, Phys. Rev. A 3, 871 (1971).

[5]W. E. Cleland *et al.*, Phys. Rev. A 5, 2338 (1972).

[6]R. D. Ehrlich *et al.*, Phys. Rev. A 5, 2357 (1972).

[7]D. E. Casperson *et al.*, Phys. Lett. 59B, 397 (1975).

[8]R. D. Stambaugh, Ph.D. thesis, Yale University, 1974 (unpublished).

[9]H. G. E. Kobrak *et al.*, Phys. Lett. 43B, 526 (1973).

[10]K. M. Crowe *et al.*, Phys. Rev. D 5, 2145 (1972).
[11]S. J. Brodsky and G. W. Erickson, Phys. Rev. 148, 26 (1966).
[12]E. R. Cohen and B. N. Taylor, J. Phys. Chem. Ref. Data 2, 663 (1973); T. W. Hänsch *et al.*, Phys. Rev. Lett. 32, 1336 (1974).
[13]T. Fulton and W. W. Repko, Phys. Rev. D 14, 1243 (1976).
[14]Vu K. Cung *et al.*, Ann. Phys. (N.Y.) 98, 516–552 (1976).
[15]M. A. B. Bég and G. Feinberg, Phys. Rev. Lett. 33, 606 (1974).
[16]J. Bailey *et al.*, Phys. Lett. 55B, 420 (1975).
[17]W. Kells *et al.*, Nuovo Cimento 35A, 289 (1976).

Precise Measurements of the Mass Attenuation of 6–25-keV Photons by Gaseous Hydrogen*

V. Yuan† and D. W. Storm
Columbia University, New York, New York 10027
(Received 28 January 1977)

We have measured the narrow-beam x-ray attenuation coefficient for gaseous hydrogen, at energies of 6.46, 14.4, 22.1, and 25.0 keV. The uncertainties are smaller than 1% for all results. The data support theoretical predictions which take account of molecular effects.

We report here some precise measurements on the attenuation of x rays in the 6–25-keV region by gaseous hydrogen. Previous attenuation measurements show large disagreements among themselves and with theoretical calculation[1] (see Fig. 1). A large part of the difficulty stems either from using hydrogen bound in hydrocarbons and a subtraction technique, or from impurities in the sample gas. The use of high-vacuum techniques and exercising great care in gas handling enabled us to maintain very much higher hydrogen purity and hence to obtain better accuracy than that of previous measurements. Our results support calculations very recently reported,[2-4] which treat the hydrogen molecule and which show rather large deviations from the atomic hydrogen calculations in the region below about 15 keV. These deviations primarily result from two-electron correlations and from binding distortion of the electron wave function.

The apparatus centers around a 3.7-m-long target pipe, which is internally collimated (3 mm in radius) and has thin Mylar windows (see Fig. 2). A radioactive source is placed at one end and a Si(Li) detector at the other. The pipe can alternately be pumped to below 10^{-6} Torr and filled with hydrogen gas up to 10 atm. In addition, the pipe is surrounded by a liquid-nitrogen bath. Cooling it to liquid-nitrogen temperatures (77°K) allows us to increase the density of target gas for a given pressure by a factor of about 4, and lowers the rate of outgassing considerably. The cooling gives a maximum hydrogen gas thickness of 1.1 g/cm^2 at 10 atm pressure. For photons of 20–30 keV, this means an attenuation of about 35%. The x rays which are not absorbed or scattered by the target produce a signal in the detector which is then amplified, shaped, and recorded in a pulse-height analyzer.

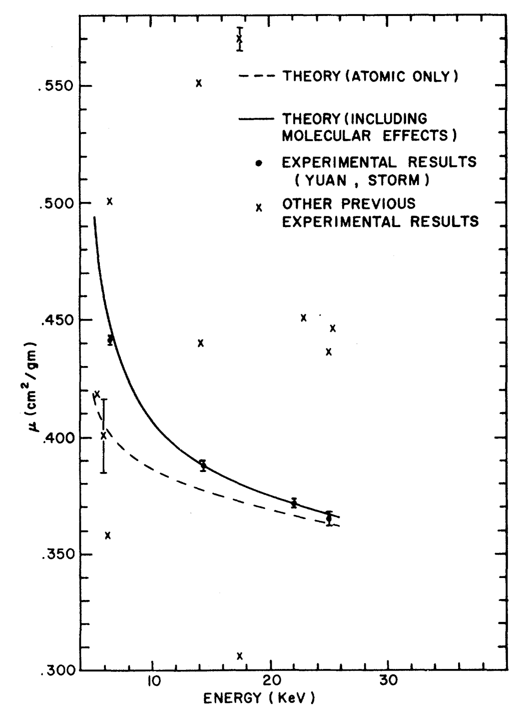

FIG. 1. Narrow-beam attenuation coefficients for gaseous hydrogen. Results of the present experiment are compared with previous measurements and with theoretical calculations. Previous data are from references compiled in Ref. 1. Calculated values are from Hubbell *et al*. (Ref. 2) with the photoelectric cross section included.